Biochimica et Biophysica Acta 1822 (2012) 233–247

Contents lists available at SciVerse ScienceDirect

Biochimica et Biophysica Acta

journal homepage: www.elsevier.com/locate/bbadis

AMPK-mediated increase of glycolysis as an adaptive response to oxidative stress in human cells: Implication of the cell survival in mitochondrial diseases

Shi-Bei Wu [a], Yau-Huei Wei [a,b,*]

[a] Department of Biochemistry and Molecular Biology, National Yang-Ming University, Taipei 112, Taiwan
[b] Department of Medicine, Mackay Medical College, New Taipei City 252, Taiwan

ARTICLE INFO

Article history:
Received 20 May 2011
Received in revised form 21 September 2011
Accepted 23 September 2011
Available online 6 October 2011

Keywords:
Mitochondrial disease
MERRF syndrome
Oxidative stress
AMPK
Glycolysis
NADPH

ABSTRACT

We report that the energy metabolism shifts to anaerobic glycolysis as an adaptive response to oxidative stress in the primary cultures of skin fibroblasts from patients with MERRF syndrome. In order to unravel the molecular mechanism involved in the alteration of energy metabolism under oxidative stress, we treated normal human skin fibroblasts (CCD-966SK cells) with sub-lethal doses of H_2O_2. The results showed that several glycolytic enzymes including hexokinase type II (HK II), lactate dehydrogenase (LDH) and glucose transporter 1 (GLUT1) were up-regulated in H_2O_2-treated normal skin fibroblasts. In addition, the glycolytic flux of skin fibroblasts was increased by H_2O_2 in a dose-dependent manner through the activation of AMP-activated protein kinase (AMPK) and phosphorylation of its downstream target, phosphofructokinase 2 (PFK2). Moreover, we found that the AMPK-mediated increase of glycolytic flux by H_2O_2 was accompanied by an increase of intracellular NADPH content. By treatment of the cells with glycolysis inhibitors, an AMPK inhibitor or genetic knockdown of AMPK, respectively, the H_2O_2-induced increase of NADPH was abrogated leading to the overproduction of intracellular ROS and cell death. Significantly, we showed that phosphorylation levels of AMPK and glycolysis were up-regulated to confer an advantage of survival for MERRF skin fibroblasts. Taken together, our findings suggest that the increased production of NADPH by AMPK-mediated increase of the glycolytic flux contributes to the adaptation of MERRF skin fibroblasts and H_2O_2-treated normal skin fibroblasts to oxidative stress.

1. Introduction

Mitochondrial diseases are mostly caused by defects in the enzymes involved in mitochondrial respiration and oxidative phosphorylation (OXPHOS) [1]. Consequently, mitochondrial dysfunction is associated with an increase of intracellular reactive oxygen species (ROS) level and a decrease of ATP content in affected tissue cells [2–4]. MERRF (myoclonic epilepsy and ragged-red fibers) syndrome is one of the major mitochondrial diseases that has been associated with an A to G transition at nucleotide position 8344 (A8344G mutation) in the $tRNA^{Lys}$ gene of mtDNA [5]. Abnormalities in the aminoacylation by $tRNA^{Lys}$ lead to premature termination of translation and result in an impairment of mitochondrial protein synthesis [6]. Biochemical studies of MERRF syndrome revealed a great reduction in the activities of respiratory enzyme Complexes I and IV in skeletal muscle and cultured skin fibroblasts accompanied with increased intracellular levels of ROS [3,7]. It has thus been suggested that oxidative stress and oxidative damage play an important role in the pathophysiology of MERRF syndrome [8,9]. Previously, we demonstrated that several nuclear DNA-encoded regulatory factors, particularly PKC-δ, were up-regulated in response to the pathogenic mtDNA mutation-elicited oxidative stress, resulting in a compensatory increase of mitochondrial biogenesis [10,11]. Nevertheless, it has remained unclear as to how cells harboring an mtDNA mutation regulate their major pathways of metabolism to cope with energy deficiency. Therefore, we investigated the energy metabolism in the primary cultures of skin fibroblasts from normal subjects and patients with MERRF syndrome.

To restore the cellular energetic status in human cells with mitochondrial dysfunction, AMP-activated protein kinase (AMPK) can switch on other ATP-generating pathways such as glycolysis and amino acid oxidation, while simultaneously switching off ATP-utilizing pathways such as fatty acid synthesis and gluconeogenesis [12]. AMPK, a heterotrimeric enzyme, is a key regulator of cellular energy metabolism consisting of the catalytic α-subunits (α1 or α2), β-regulatory subunits (β1 or β2) and AMP binding subunits (γ1, γ2 or γ3) [13]. It has been reported that AMPK is activated by phosphorylation of the catalytic subunits at Thr^{172} [14], which is mediated by a tumor suppressor, LKB1 kinase, and several Ca^{2+}/calmodulin-dependent protein kinases (CaMKs) [15,16]. Recent studies also showed that AMPK can be activated by reactive oxygen/nitrogen species (ROS/RNS) [17]. The

* Corresponding author at: Department of Biochemistry and Molecular Biology, National Yang-Ming University, Address: No. 155, Li-Nong St., Sec. 2, Taipei 112, Taiwan. Tel.: +886 2 28267118; fax: +886 2 28264843.
E-mail addresses: joeman@ym.edu.tw, joeman@mmc.edu.tw (Y.-H. Wei).

0925-4439/$ – see front matter © 2011 Elsevier B.V. All rights reserved.
doi:10.1016/j.bbadis.2011.09.014

activation of AMPK by ultraviolet (UV) irradiation, hydrogen peroxide (H_2O_2), nitric oxide (NO) and peroxynitrite ($•ONOO^-$), respectively, has been reported in various human cell lines [18–20]. However, it is unknown as to whether AMPK activation induced by ROS or RNS has an effect on the major pathways of energy metabolism in skin fibroblasts.

It has been reported that the redistribution of glucose metabolites is involved in the regulation of antioxidant defense system [21,22]. The carbon flux through the oxidative branch of the pentose phosphate pathway (PPP) is viewed as a part of the antioxidant defense system due to the generation of reduced nicotinamide adenine dinucleotide phosphate (NADPH) by glucose 6-phosphate dehydrogenase (G6PD) [23]. NADPH is considered as a critical source of reducing equivalent, which contributes to the maintenance of the antioxidant defense capability and glutathione (GSH) regeneration [24]. The NADPH-dependent antioxidant enzymes including the thioredoxin and glutaredoxin systems play important roles in the maintenance of redox homeostasis owing to the regulation of thiol-disulfide exchange [25,26]. Although manipulating the carbohydrate source of the culture medium can interfere with the intracellular NADPH production via the PPP [27], it remains unclear whether the increase of the glycolytic flux can contribute to an increase of the intracellular NADPH content of human cells.

In order to unravel the molecular mechanism involved in the regulation of energy metabolism for the cell survival under oxidative stress, we first investigated the alteration of glucose metabolism in sub-lethal H_2O_2-treated normal human skin fibroblasts (CCD-966SK cells) and in the primary culture of skin fibroblasts from MERRF patients. We observed that an increase of the glycolytic flux was regulated by AMPK, which was accompanied by elevation of intracellular NADPH and GSH contents in skin fibroblasts against oxidative stress. We consider that AMPK-mediated metabolic switch and antioxidant response are essential for the cell survival in affected tissues harboring a pathogenic mtDNA mutation, which may play an important role in the pathophysiology of mitochondrial diseases such as MERRF syndrome.

2. Materials and methods

2.1. Cell cultures

The primary cultures of skin fibroblasts from normal subjects (N1–N4, average age of 21.3 ± 3.8 years), MERRF patients (M1–M4, average age of 19.3 ± 5.5 years) and a normal human skin fibroblast cell line (CCD-966SK, ATCC number: CRL-1881) were cultured at 37 °C in a humidified chamber filled with 5% CO_2. Cells were cultured in Dulbecco's modified Eagle's medium (DMEM, Gibco, Invitrogen Corp., Carlsbad, CA, USA) containing 10% fetal bovine serum (FBS, Biological Industries, Kibbutz Beit Haemek, Israel) and antibiotics (Biological Industries, Kibbutz Beit Haemek, Israel) composed of 100 U/ml penicillin G and 100 μg/ml streptomycin sulfate, respectively. The primary cultures of skin fibroblasts were used at passages 3 to 5 and the molecular diagnosis of MERRF skin fibroblasts revealed an A8344G mutation in mtDNA (M1: 53.6 ± 7.9%, M2: 78.3 ± 7.2%, M3: 84.2 ± 3.8%, M4: 72.2 ± 11.3%), but not in normal skin fibroblasts [11].

2.2. Chemicals and antibodies

An AMPK inhibitor (Compound C), *N*-acetylcysteine (NAC), 2'-deoxy-D-glucose (2DG), antimycin A (AnA), and 6-aminonicotinamide (6AN) were purchased from Sigma-Aldrich Chemical Co. (St. Louis, MO, USA) and H_2O_2 was procured from Merck (Darmstadt, Germany). The antibodies against glycolytic enzymes (GPI, PFK1, PFK2, LDH, PDH, PDK and phosphorylated PFK2 at Ser^{466}) were supplied by Santa Cruz Biotechnology (Santa Cruz, CA, USA), and GLUT1, HK II, GAPDH and β-actin antibodies were purchased from Millipore (Billerica, MA, USA). The antibodies specific to AMPK-1α and phosphorylated AMPK-1α (Thr^{172}) were acquired from Cell Signaling Technologies (Beverly, MA, USA). The antibodies against G6PD, GPx-1, GR, Trx-1, and Prx-1, respectively, were purchased from AbFrontier Co., Ltd. (Seoul, Korea).

2.3. Knockdown of AMPK-1α

The small hairpin RNA (shRNA) plasmids for the AMPK-1α gene (shAMPK) and luciferase control gene (shLuci) were obtained from the RNAi Core Facility at Academia Sinica, Taipei, Taiwan. The shLuci and shAMPK-1α constructs were made by using the pLKO plasmid (http://www.addgene.org/plko) and the target sequences were 5′-CAAATCACAGAATCGTCGTAT-3′ and 5′-GCCTGGCTATGGAACTAAATA-3′, respectively. With TurboFect™ in vitro transfection reagent (Fermentas Life Science, Vilnius, Lithuania), 2 μg/ml of shAMPK could effectively abolish the AMPK-1α expression in human skin fibroblasts at 24, 48, and 72 h, respectively, according to the protocol recommended by the manufacturer.

2.4. Determination of intracellular H_2O_2 content

The intracellular H_2O_2 content in skin fibroblasts was measured by incubating cells with the probe 2′,7′-dichlorofluorescin diacetate (DCFH-DA) at 20 μM, 37 °C for 20 min (Molecular Probes, Eugene, OR, USA). After trypsinization, cells were resuspended in 0.5 ml of PBS buffer (pH 7.4), and subjected to analysis on a flow cytometer (Model EPICS XL-MCL, Beckman-Coulter, Miami, FL, USA). The excitation wavelength was set at 488 nm and the intensity of emitted fluorescence of a total of 10,000 cells at 525 nm was recorded on channel FL1. Data were acquired and analyzed using the EXPO32™ software (Beckman-Coulter, Miami, FL, USA), and the intracellular H_2O_2 contents in the treated cells are presented as relative values compared to that of the cells without H_2O_2 treatment.

2.5. Measurement of bioenergetic parameters

An XF24 Analyzer (Seahorse Bioscience, North Billerica, MA, USA) was used to measure the bioenergetic function of the primary culture of skin fibroblasts [28]. The XF24 Analyzer can create a transient 7-μl chamber to the cells cultured in a 24-well microplate, and the oxygen consumption rate (OCR) and extracellular acidification rate (ECAR) were monitored real-time in an incubation chamber at 37 °C. Briefly, a seeding density of 16,000 skin fibroblasts per well was chosen and the culture medium was replaced 1 h prior to measurement by the assay medium that contained un-buffered DMEM (pH 7.4). The program of Seahorse XF24 Analyzer was set according to the manufacturer's recommendation and the data are expressed in pmol/min/10^4 cells for OCR and in mpH/min/10^4 cells for ECAR to allow comparison between independent experiments.

2.6. Determination of mitochondrial oxygen consumption

The rate of mitochondrial oxygen consumption was measured on an Oxygen Meter 782 (Strathkelvin Instruments, Scotland, UK) with a water circulation system to maintain the assay condition at 37 °C as described previously [29]. Briefly, about 10^6 cells were suspended in 330 μl assay buffer (125 mM sucrose, 65 mM KCl, 2 mM $MgCl_2$, 20 mM phosphate buffer, pH 7.2), and then transferred to the incubation chamber. After recording the rate of oxygen consumption for 5 min, 20 μl of 25 mM KCN was added to the chamber to inhibit mitochondrial respiration and the non-mitochondrial oxygen consumption rate was recorded for another 3 min. The rate of oxygen consumption was calculated by the SI 782 Oxygen System software version 3.0, and was normalized by the cell number after subtracting the rate of non-mitochondrial oxygen consumption.

2.7. Measurement of intracellular ATP content

The intracellular ATP content in skin fibroblasts was measured by the Bioluminescent Somatic Cell Assay Kit (Sigma-Aldrich) according to a method described previously [30]. Briefly, an aliquot of 50 μl cell suspension (10^6 cells) was mixed with 150 μl Somatic Cell Releasing Reagent to release the intracellular ATP. One half (100 μl) of the mixture was then transferred to a black 96-well plate (OptiPlate™, Packard

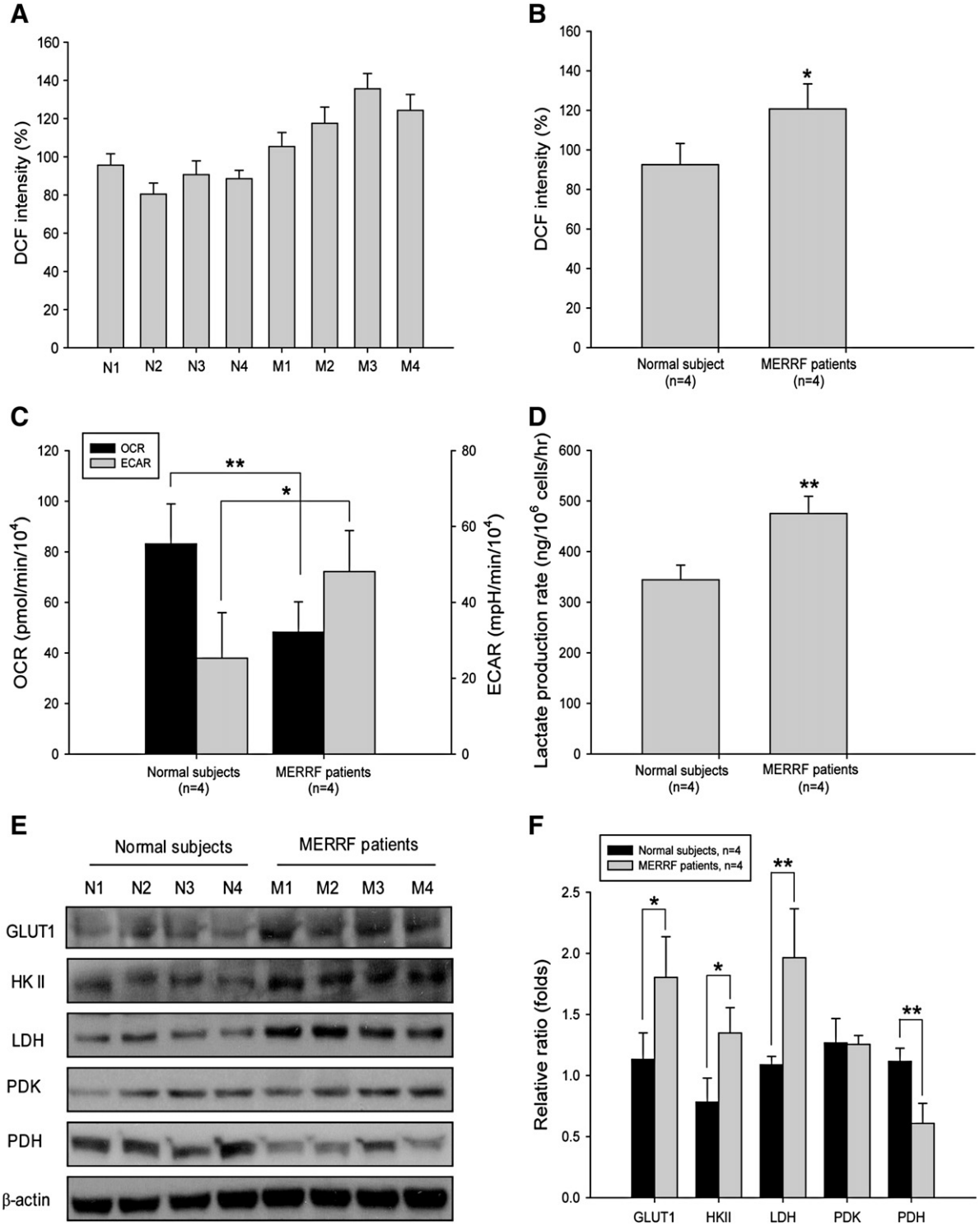

Fig. 1. Increase of oxidative stress and anaerobic glycolysis in skin fibroblasts from patients with MERRF syndrome. The primary culture of skin fibroblasts from four MERRF patients (M1–M4) and four age-matched normal skin fibroblasts (N1–N4) were used. (A) Intracellular H_2O_2 content was determined by DCF staining and (B) the mean values of the DCF intensity in the skin fibroblasts of normal subjects and in MERRF skin fibroblasts are shown in histogram. (C) The mean values of OCR and ECAR were measured in real-time by a Seahorse XF24 Analyzer and (D) the mean values of lactate production rate were determined in skin fibroblasts from normal subjects and MERRF patients, respectively. (E) By Western blot, the expression of glycolytic enzymes in skin fibroblasts of normal subjects and MERRF skin fibroblasts were determined, respectively. (F) By densitometric analysis from three independent Western blots, the expression levels of glycolytic enzymes were normalized to the corresponding β-actin expression level. The representative histogram was constructed on the basis of the mean values of proteins expression levels in skin fibroblasts of normal subjects and MERRF skin fibroblasts, respectively. Data are presented as means ± S.D. of the results from three independent experiments (*, $p<0.05$, ** $p<0.01$ vs. the indicated group).

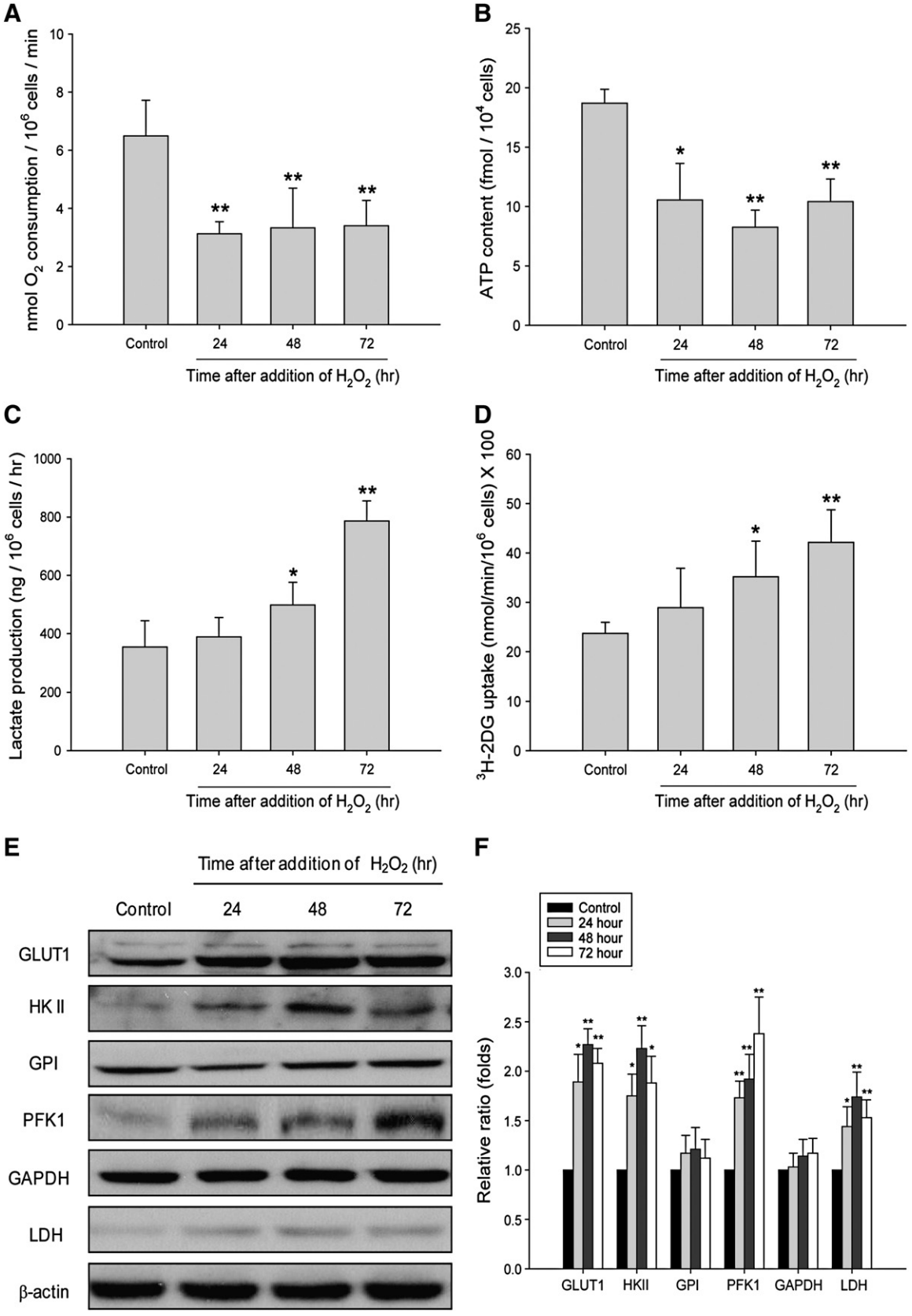

Fig. 2. Metabolic shift from mitochondrial respiration to anaerobic glycolysis in H_2O_2-treated normal skin fibroblasts. After exposure of CCD-966SK cells with 250 μM H_2O_2 for 90 min, the cells were washed with PBS and incubated with the complete culture medium for 24, 48 and 72 h, respectively. (A) The rate of mitochondrial oxygen consumption, (B) the intracellular ATP content, (C) the rate of lactate production, and (D) the rate of [^{3}H]-2-deoxy-glucose ([^{3}H]-2DG) uptake were determined. (E) Western blot for the measurement of the expression of the glycolytic enzymes in CCD-966SK cells after induction with H_2O_2 stress for 24, 48 and 72 h, respectively. (F) The representative histogram was constructed on the basis of the results from three independent Western blots and data are presented as means ± S.D. (*, $p<0.05$, **, $p<0.01$ vs. the indicated group).

Biosciences, Groningen, The Netherlands), which contained 100 μl ATP Assay Mix. The luminescence intensity was then measured by the Victor$^2_{TM}$ 1420 multilabel counter machine (PerkinElmer Life Sciences Inc., Boston, MA, USA). The ATP standards ranging from 0 to 300 pmol were used and each ATP value was normalized by the cell number.

2.8. Determination of the glucose uptake rate

The glucose uptake rate of skin fibroblasts was measured by the addition of a [^{3}H]-labeled glucose analog, 2′-deoxy-D-[2,6-^{3}H] glucose ([^{3}H]-2DG) to the assay medium. Briefly, cells were cultured in a 6-well plate and washed with the Krebs–Ringer phosphate buffer (KRP, pH 7.4) containing 130 mM NaCl, 5 mM KCl, 1.3 mM $CaCl_2$, 1.3 mM $MgSO_4$, and 10 mM Na_2HPO_4. After washing with the KRP, the 6-well plate was placed in a shaker maintained at 37 °C with a water bath. The reaction was carried out by the addition of [^{3}H]-2DG (final concentration at 0.2 mM, 7.5 mCi/μmol) for 20 min at 37 °C and stopped by the addition of ice-cold 20 mM glucose solution for another 5 min. The solution was then removed by suction and rapidly washed three times with ice-cold PBS. Finally, 1 ml of 2% SDS was added to the plate and the extract was counted for the radioactivity by Tri-Carb 2900TR equipped with a Beta counter (GMI Inc., Ramsey, MN, USA).

2.9. Determination of lactate production rate

The rate of lactate production was measured by a Lactate Reagent kit (Trinity Biotech, Bray, Ireland). Briefly, cells in a 6-well plate were incubated with the fresh culture medium for 8 h, and an aliquot of 10 μl of medium was then transferred to a 96-well plate to mix with the Lactate Reagent. The absorbance at 540 nm of a product generated by the reaction was measured by an ELISA reader PowerWavex 340 (Bio-Tek Instruments, Winooski, VT, USA). The amount of lactate produced by cells during the incubation period of time was calculated according to the standard curve constructed by lactate standards. The rate of lactate production was normalized by the cell number and divided by the length of incubation time.

2.10. Western blot analysis

An aliquot of 50 μg proteins was separated on 10% SDS-PAGE and blotted onto a piece of the PVDF membrane (Amersham-Pharmacia Biotech Inc., Buckinghamshire, UK). After blocking by 5% skim milk in the TBST buffer (50 mM Tris–HCl, 150 mM NaCl, 0.1% Tween 20, pH 7.4) for 1 h, the membrane was incubated for another 1 h with a primary antibody at room temperature. After washing 3 times with the TBST, the blot was incubated with a horseradish peroxidase (HRP)-conjugated secondary antibody for 1 h at room temperature. An enhanced chemiluminescence detection kit (Amersham-Pharmacia Biotech Inc., Buckinghamshire, UK) was used to detect the protein signals with a Fuji X-ray film (Fuji Film Corp., Tokyo, Japan), and the signals were quantified by ImageScanner III with the LabScan 6.0 software (GE Healthcare BioSciences Corp., Piscataway, NJ, USA).

2.11. Determination of cell viability

Cell viability was measured by the Trypan blue exclusion assay, and the cells were counted by using a haemocytometer. The number of viable cells was determined on the basis of their exclusion of 0.4% Trypan blue (Sigma-Aldrich, St. Louis, MO, USA). The relative cell viability was normalized by the value of cells without H_2O_2 treatment, and is expressed as mean ± S.D. of the results from three independent experiments.

2.12. Determination of the intracellular NADPH content

Intracellular NADPH content was measured by an NADPH quantification kit (K347-100, BioVision Inc., Mountain View, CA, USA). Briefly,

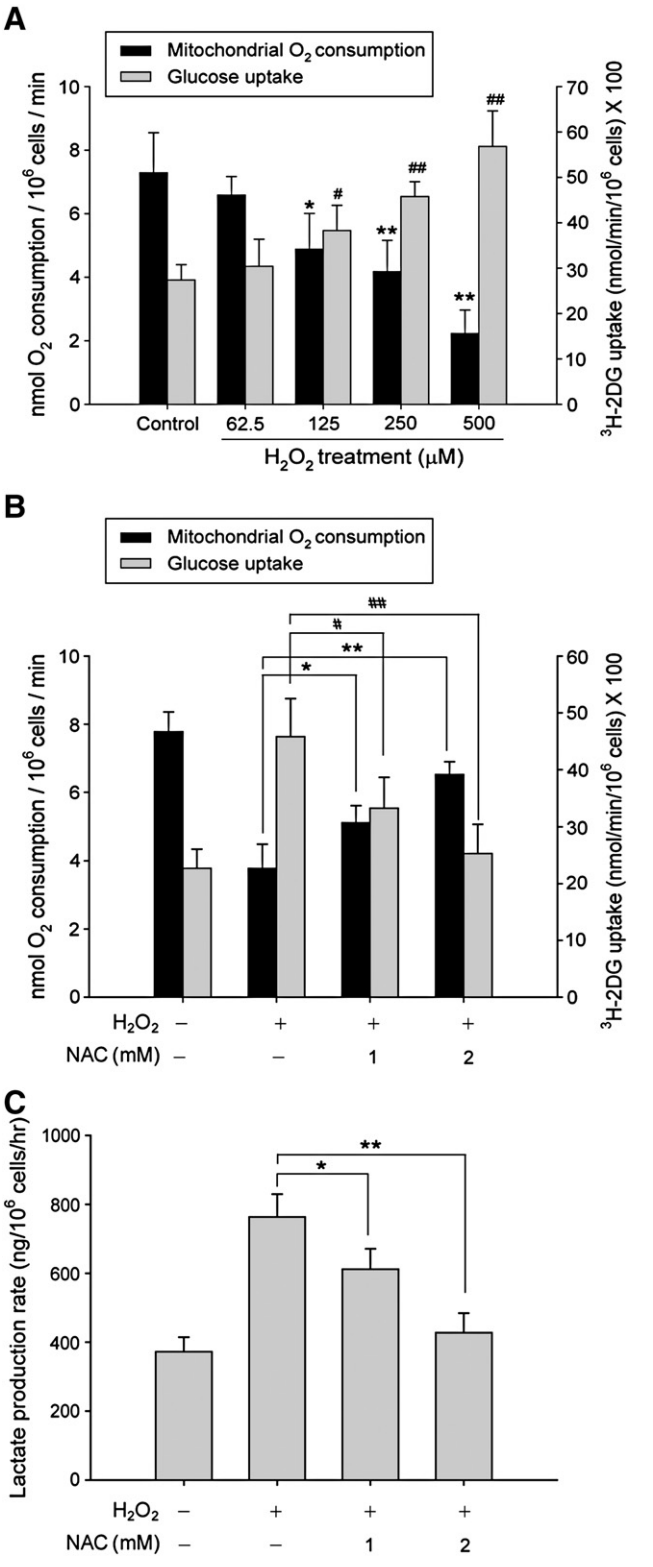

Fig. 3. Enhanced glycolytic flux as a response to H_2O_2 toxicity in normal skin fibroblasts. (A) After treatment of CCD-966SK cells with various concentrations of H_2O_2, the rates of mitochondrial oxygen consumption and [^{3}H]-2DG uptake in CCD-966SK cells were determined at 72 h, respectively. (B) By pre-treatment of CCD-966SK cells with 1 and 2 mM NAC followed by addition of 250 μM H_2O_2, the rates of mitochondrial oxygen consumption, the rates of [^{3}H]-2DG uptake and (C) lactate production were determined at 72 h, respectively. Data are presented as means ± S.D. of the results from three independent experiments (* and $^{\#}$, $p<0.05$, ** and $^{\#\#}$, $p<0.01$ vs. the indicated group).

about 10^6 cells were harvested by trypsinization and lysed in 50 μl of 0.1 N NaOH followed by neutralization with the addition of 50 μl of 0.1 N HCl. An aliquot of 900 μl extraction buffer was added to the sample and incubated at 4 °C for 20 min. The sample was then incubated at 60 °C for 1 h to completely destroy $NADP^+$, leaving NADPH intact. After incubation of the sample with the NADPH developer buffer at room temperature for 1 h, the absorbance at 450 nm was measured by an ELISA reader PowerWavex 340 (Bio-Tek Instruments, Winooski, VT, USA). A standard curve for NADPH (0–100 pmol) was established and the intracellular NADPH content was calculated and normalized by the cell number.

2.13. Measurement of intracellular GSH contents

The amount of GSH was measured by the Bioxytech GSH-400 quantification kit (Oxis Internation, Inc., Portland, OR). Briefly, about 10^6 cells were harvested by trypsinization and lysed in 350 μl of 5% metaphosphoric acid (MPA) followed by centrifugation at 3,000 × *g* for 10 min at 4 °C. The GSH content was determined from 50 μl of MPA extract (supernatant) which was incubated in the presence of 5-5′-dithiobis-2-nitrobenzoic acid (DTNB), NADPH and GR according to the manufacturer's protocol. The change in absorbance at 400 nm over 3 min was measured on a Hitachi U-3410 UV/VIS spectrophotometer (Hitachi High Technologies Corp., Japan) for both samples and standards (0 to 3.0 μmol of GSH). The GSH level was normalized by the protein concentration and expressed as nmol/mg protein.

2.14. Statistical analysis

Statistical analysis was performed by using the Microsoft Excel 2007 statistical package and the data are presented as means ± S.D. of the results obtained from three independent experiments. The significance level of the difference between the control and the experimental groups was determined by the Student's t test. A difference was considered statistically significant when the p value < 0.05 (* and #) and p value < 0.01 (** and ##), respectively.

3. Results

3.1. Increased oxidative stress and anaerobic glycolysis in skin fibroblasts from patients with MERRF syndrome

The intracellular H_2O_2 content and the bioenergetic function were determined for the primary cultures of skin fibroblasts from four age-matched normal subjects (N1–N4, normal skin fibroblasts) and four

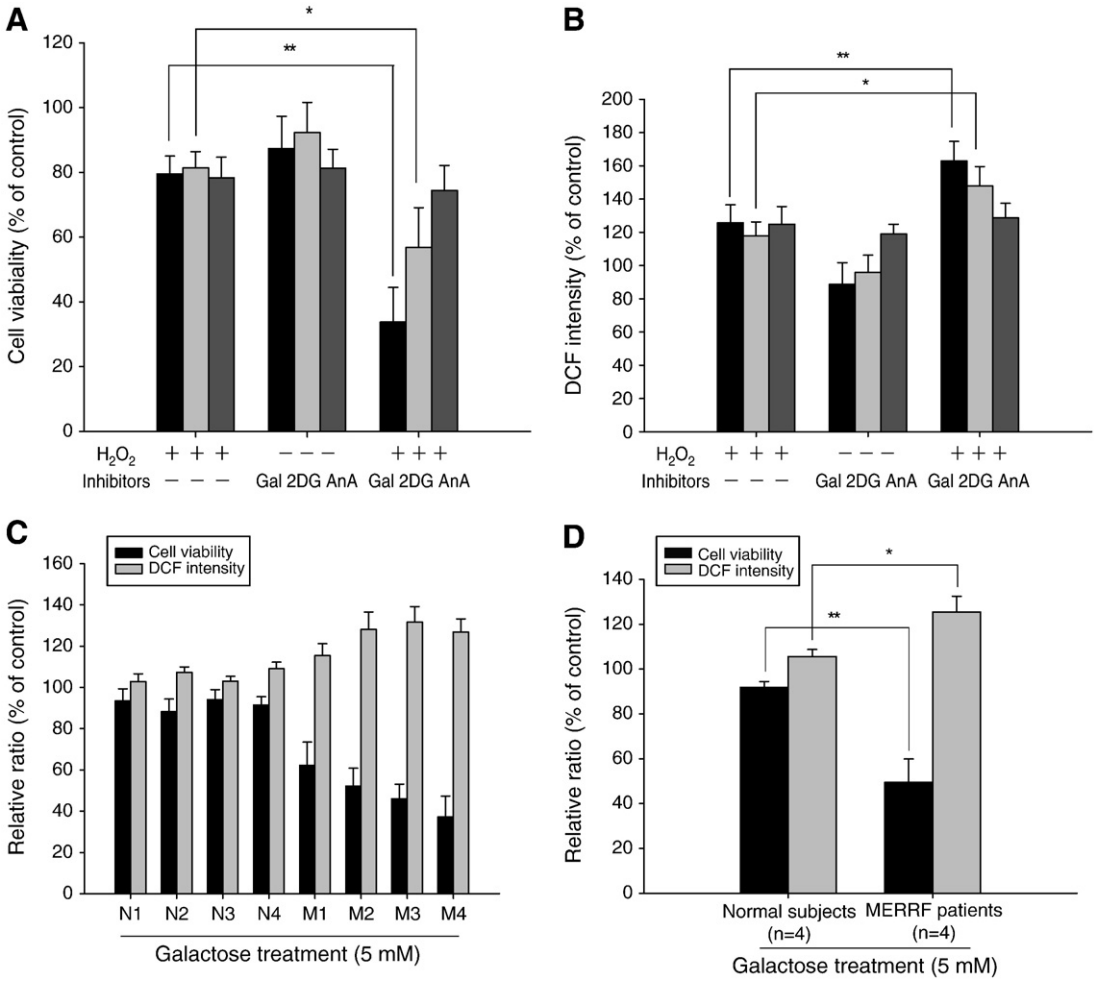

Fig. 4. Essential of increased glycolytic flux for normal skin fibroblasts to cope with H_2O_2 and for the survival of MERRF skin fibroblasts. After induction of oxidative stress by 250 μM H_2O_2 at 24 h, CCD-966SK cells were incubated with 5 mM galactose in a glucose-free medium, 20 mM 2DG (an HK inhibitor) and 1 mM AnA (a Complex III inhibitor) in a glucose-containing medium, respectively, for another 48 h. (A) The cell viability was determined by Trypan blue exclusion assay and (B) the intracellular H_2O_2 content was measured by DCF staining. Data were normalized to the control without H_2O_2 treatment. (C) The primary cultures of skin fibroblasts from normal subjects (n = 4) and MERRF patients (n = 4) were incubated, respectively, with 5 mM galactose in a glucose-free medium followed by determination of the cell viability and the intracellular H_2O_2 content at 48 h and (D) the mean values of cell viability and intracellular H_2O_2 content are shown in the histogram. Data are presented as means ± S.D. of the results from three independent experiments (*, $p<0.05$, **, $p<0.01$ vs. the indicated group).

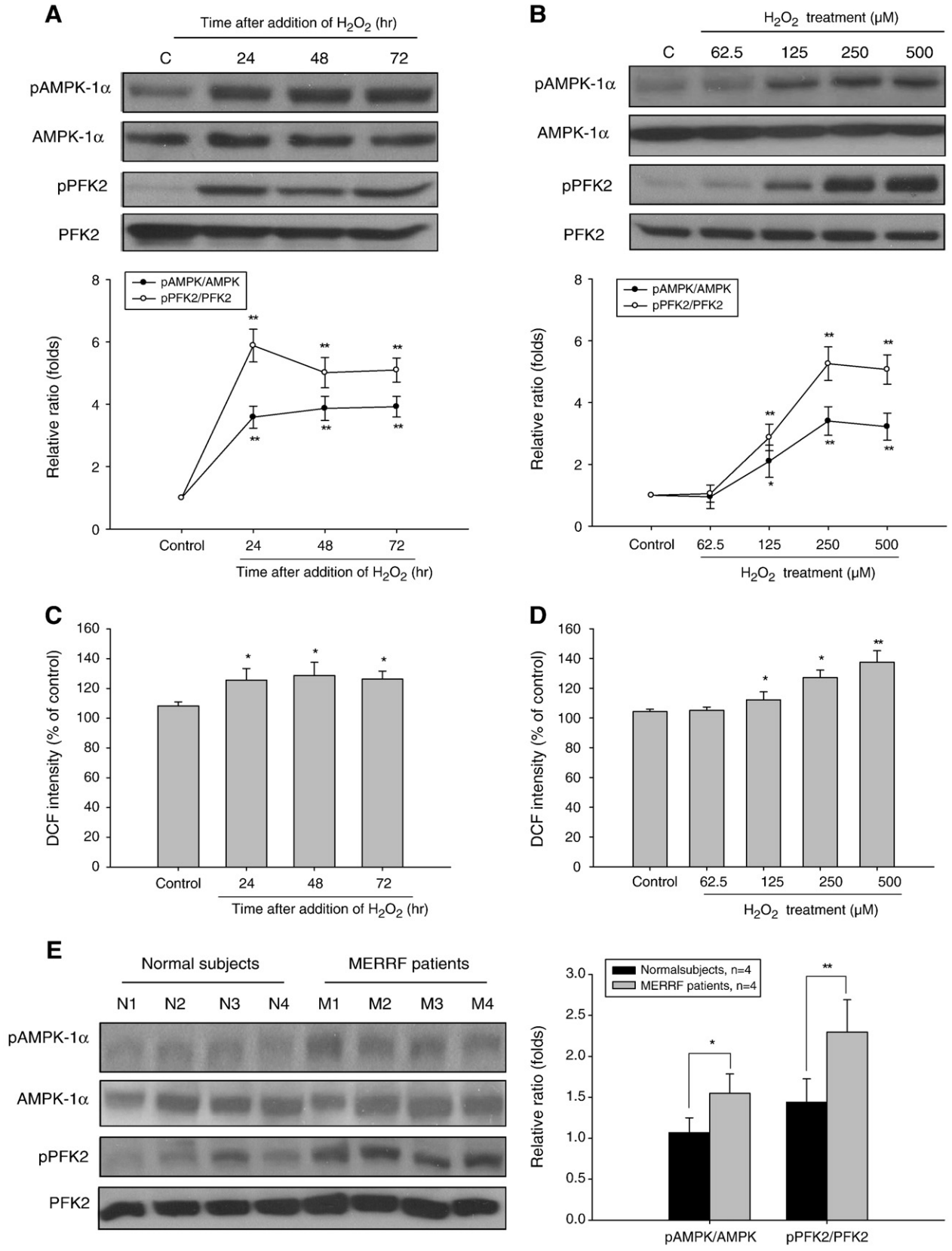

Fig. 5. Up-regulation of the phosphorylated AMPK and PFK2 in H_2O_2-treated normal skin fibroblasts and MERRF skin fibroblasts. (A) By Western blot, the phosphorylation levels of AMPK-1α and PFK2 were evaluated after treatment of CCD-966SK cells with 250 μM H_2O_2 at 24, 48 and 72 h, respectively. (B) Phosphorylated AMPK-1α and PFK2 in CCD-966SK cells was examined after treatment of cells with various concentrations of H_2O_2 at 72 h. By densitometric analysis from three independent Western blots, the ratios of pAMPK-1α / AMPK-1α and pPFK2/PFK2, respectively, are shown in the following panel. (C) After addition of 250 μM H_2O_2 to CCD-966SK cells for 90 min, the intracellular H_2O_2 content was measured at 24, 48 and 72 h. (D) The intracellular H_2O_2 content was determined at 72 h after treatment of CCD-966SK cells with different concentrations of H_2O_2 for 90 min. (E) By Western blot, the phosphorylation levels of AMPK-1α and PFK2 were determined in the primary culture of skin fibroblasts from normal subjects (n = 4) and MERRF patients (n = 4). Densitometric scan was analyzed from three independent Western blots for the ratios of pAMPK-1α/AMPK-1α and pPFK2/PFK2 and the results are shown in the right panel. Data are presented as means ± S.D. of the results from three independent experiments (*, $p<0.05$, **, $p<0.01$ vs. the indicated group).

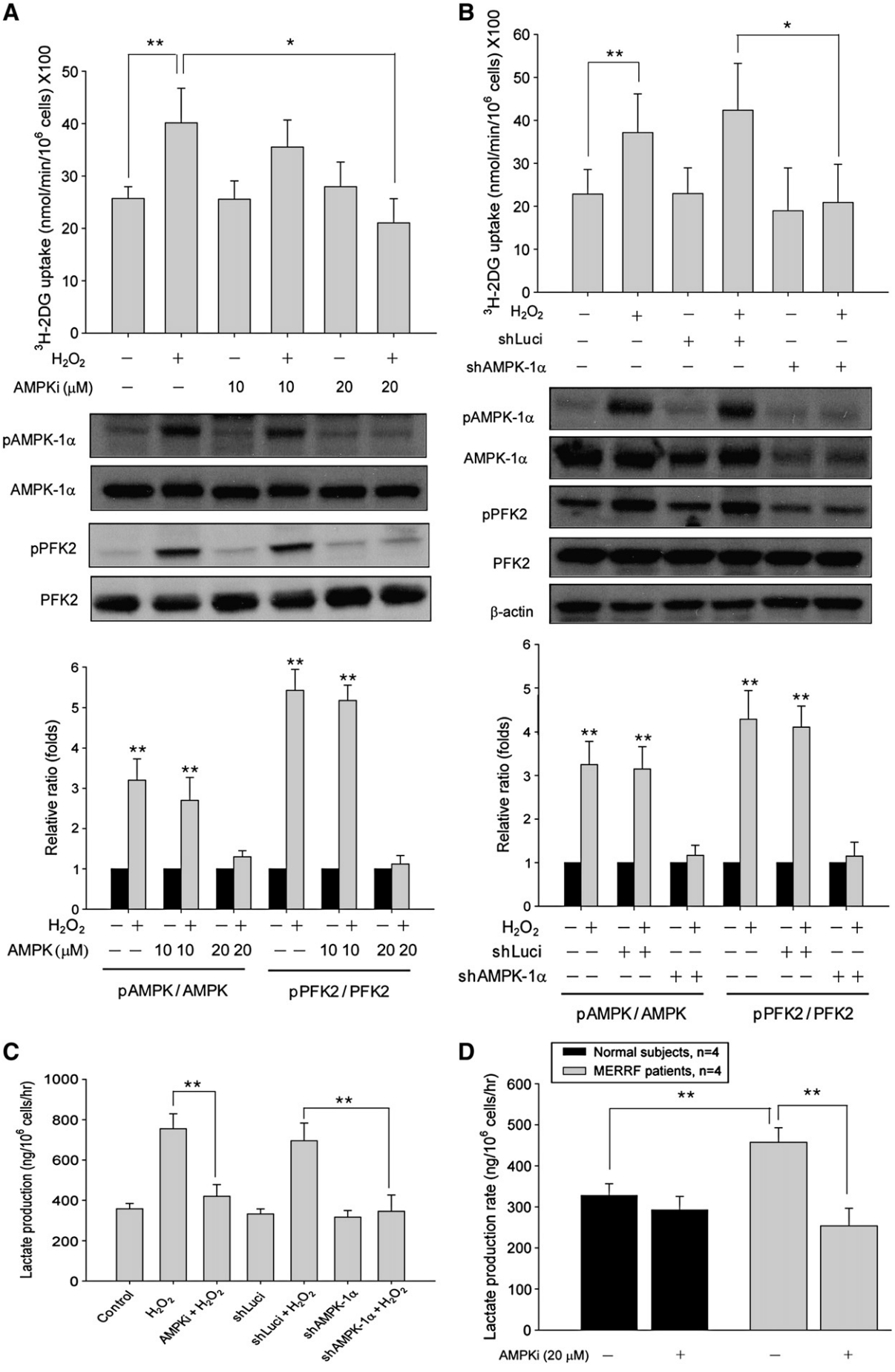
A
B
C
D
^{3}H-2DG uptake (nmol/min/10^6 cells) X100
H$_2$O$_2$
AMPKi (μM)
shLuci
shAMPK-1α
pAMPK-1α
AMPK-1α
pPFK2
PFK2
β-actin
Relative ratio (folds)
pAMPK / AMPK
pPFK2 / PFK2
Lactate production (ng/10^6 cells/hr)
Control
AMPKi + H$_2$O$_2$
shLuci + H$_2$O$_2$
shAMPK-1α
shAMPK-1α + H$_2$O$_2$
Normal subjects, n=4
MERRF patients, n=4
Lactate production rate (ng/10^6 cells/hr)
AMPKi (20 μM)

MERRF patients (M1–M4, MERRF skin fibroblasts), respectively. The results showed that the intracellular H_2O_2 contents in MERRF skin fibroblasts were significantly higher than those of controls (Fig. 1A and B). In addition, by using the Seahorse XF24 Analyzer, we found a decrease of OCR, but an increase of ECAR in MERRF skin fibroblasts as compared with those of normal skin fibroblasts (Fig. 1C). Moreover, the rate of lactate production was significantly increased in MERRF skin fibroblasts as compared with normal subjects (Fig. 1D). On the other hand, Western blot revealed that the expression levels of glycolytic enzymes including lactate dehydrogenase (LDH), hexokinase type II (HK II) and glucose transporter 1 (GLUT1) were increased, but the expression of pyruvate dehydrogenase (PDH) was decreased in MERRF skin fibroblasts as compared with those of normal controls (Fig. 1E and F).

3.2. Metabolic shift from mitochondrial respiration to anaerobic glycolysis in H2O2-treated normal skin fibroblasts

Based on the observed increase in the intracellular H_2O_2 contents and glycolytic phenotype in MERRF skin fibroblasts (Fig. 1), we reasoned that energy metabolism in skin fibroblasts may be perturbed by oxidative stress. In order to unravel the molecular mechanism involved in the regulation of glucose metabolism under oxidative stress, we treated the normal human skin fibroblasts (CCD-966SK cells) with sub-lethal doses of H_2O_2 and examined the alterations of mitochondrial respiration and anaerobic glycolysis. After treatment of CCD-966SK cells with sub-lethal doses of H_2O_2 (62.5, 125, 250 and 500 μM) for 90 min, no significant changes of caspase 3 activity and the proportion of sub-G_0 cells were found at 72 h (Supplementary Fig. 1). In addition, after treatment of CCD-966SK cells with 250 μM H_2O_2 for 90 min, we found that the rate of mitochondrial oxygen consumption and intracellular ATP levels were substantially decreased at 24, 48 and 72 h, respectively (Fig. 2A and B). Nevertheless, the rates of lactate production and the [^{3}H]-2DG uptake by CCD-966SK cells were significantly increased at 48 and 72 h after exposure of H_2O_2 (Fig. 2C and D). Furthermore, by using the Seahorse XF24 Analyzer, we found that the OCR was remarkably decreased at 24 h, but the ECAR was significantly increased at 48 and 72 h after addition of H_2O_2 to CCD-966SK cells (Supplementary Fig. 2). Moreover, as revealed by Western blot, the protein expression levels of glycolytic enzymes including GLUT1, HK II, PFK1 and LDH, respectively, were increased after treatment of CCD-966SK cells with 250 μM H_2O_2 at 24, 48 and 72 h, respectively (Fig. 2E and F). On the other hand, we also observed that by treatment of CCD-966SK cells with 125 μM or higher doses of H_2O_2 for 90 min, the rate of mitochondrial oxygen consumption was decreased and the rate of [^{3}H]-2DG uptake was increased in a dose-dependent manner at 72 h (Fig. 3A). However, by pre-treatment of CCD-966SK cells with 1 and 2 mM *N*-acetylcysteine (NAC) for 1 h, followed by exposure to 250 μM H_2O_2 for 90 min, the H_2O_2-induced increase in the rates of [^{3}H]-2DG uptake and lactate production were attenuated at 72 h (Fig. 3B and C).

3.3. Contribution of anaerobic glycolysis to the survival of H_2O_2-treated normal skin fibroblasts and MERRF skin fibroblasts

In order to examine whether the enhanced glycolysis is essential for cell survival under oxidative stress, we inhibited glycolysis and determined the cell viability. After addition of 250 μM H_2O_2 to CCD-966SK cells for 24 h, we replaced the glucose-supplemented DMEM with a galactose-containing DMEM followed by culture of the cells for another 48 h. Upon inhibition of glycolysis, the cells could obtain their energy from oxidation of a non-carbohydrate source such as glutamine in mitochondria [21]. The results showed that the cell viability was substantially decreased in H_2O_2-treated CCD-966SK cells that were cultured in a glucose-free medium supplemented with 5 mM galactose (Fig. 4A). Besides, after exposure of CCD-966SK cells to H_2O_2 for 24 h, we treated the cells with 2′-deoxy-glucose (2DG, an HK inhibitor) and antimycin A (AnA, a Complex III inhibitor) in a glucose-containing medium, respectively, for another 48 h. The results indicated that the cell viability was further decreased in H_2O_2-treated CCD-966SK cells under the inhibition of glycolysis by 2DG, but inhibition of mitochondrial function by AnA exerted little effect on cell viability (Fig. 4A). Moreover, we observed that the H_2O_2-induced intracellular ROS level in CCD-966SK cells was further elevated only by the inhibition of glycolysis (Fig. 4B). On the other hand, we inhibited glycolysis in the primary culture of skin fibroblasts from MERRF patients (n = 4) and normal subjects (n = 4), respectively, by addition with 5 mM galactose in a glucose-free medium for 48 h. The results showed that the cell viability was lower and the intracellular ROS level was higher in MERRF skin fibroblasts as compared with those of normal skin fibroblasts (Fig. 4C and D).

3.4. Increase of glycolytic flux by AMPK activation in H_2O_2-treated normal skin fibroblasts and MERRF skin fibroblasts

It has been shown that activation of AMPK is involved in the regulation of glycolysis in human cells by phosphorylating its downstream target, PFK2 against oxidative stress [31]. Hence, we investigated whether AMPK activation directly participates in the regulation of energy metabolism in skin fibroblasts under oxidative stress. As revealed by Western blot, phosphorylation levels of AMPK-1α and PFK2 were induced at 24, 48, and 72 h, respectively, after incubation of CCD-966SK cells with 250 μM H_2O_2 for 90 min (Fig. 5A). Besides, by treatment of CCD-966SK cells with H_2O_2 at 125 μM or higher concentrations for 90 min, the phosphorylated forms of AMPK-1α and PFK2 were increased at 72 h in a dose-dependent manner (Fig. 5B). On the other hand, we observed the accumulation of ROS in H_2O_2-treated CCD-966SK cells at 24, 48 and 72 h (Fig. 5 C). In addition, the intracellular ROS content was increased in a dose-dependent manner after addition of various concentrations of H_2O_2 to CCD-966SK cells at 72 h (Fig. 5D). Finally, we examined the activation of AMPK and PFK2 in MERRF skin fibroblasts and the results showed that the ratios of the phosphorylated forms of AMPK-1α and PFK2 relative to AMPK-1α and PFK2, respectively, were substantially increased in MERRF skin fibroblasts as compared with those of the normal skin fibroblasts (Fig. 5E).

To clarify whether the H_2O_2-induced AMPK-1α activation contributes to the enhanced glycolysis in skin fibroblasts, we pre-treated CCD-966SK cells with Compound C, an AMPK inhibitor (AMPKi) followed by exposure to H_2O_2. The results showed that by pre-treatment of CCD-966SK cells with 20 μM AMPKi for 1 h, the H_2O_2-induced phosphorylation of AMPK-1α and PFK2 was abrogated at 72 h and the rate of [^{3}H]-2DG uptake was significantly diminished (Fig. 6A). In addition, to address specifically the role of AMPK, we transfected the CCD-966SK cells with a shRNA of AMPK-1α to knockdown AMPK-1α. Western blot revealed that the expression of AMPK-1α was decreased in cells transfected with AMPK-1α-shRNA (shAMPK-

Fig. 6. Regulation of glycolytic flux by AMPK in H_2O_2-treated normal skin fibroblasts and MERRF skin fibroblasts. (A) By pre-treatment of CCD-966SK cells with 10 or 20 μM AMPK inhibitor (AMPKi) for 1 h, followed by addition of 250 μM H_2O_2 for 90 min, the rate of [^{3}H]-2DG uptake was determined and the phosphorylation levels of AMPK-1α and PFK2 were analyzed by Western blot at 72 h. (B) After treatment with 250 μM H_2O_2 in shLuci- and shAMPK-1α-transfected cells for 90 min, the rate of [^{3}H]-2DG uptake was determined and the phosphorylation levels of AMPK-1α and PFK2 were analyzed by Western blot at 72 h. By densitometric analysis of three independent Western blots from A and B, the ratios of pAMPK-1α /AMPK-1α and pPFK2/PFK2 are shown in the following panels, respectively. (C) Upon inhibition of AMPK activation in CCD966SK cells by pre-treatment of the cells with AMPKi for 1 h and by knockdown of AMPK-1α gene, respectively, followed by addition of 250 μM H_2O_2 for 90 min, the rate of lactate production was determined. (D) After treatment of the primary culture of skin fibroblasts from normal subjects (n = 4) and MERRF patients (n = 4) with 20 μM AMPKi for 24 h, the mean values of lactate production rates were determined, respectively. Data are presented as means ± S.D. of the results from three independent experiments (*, $p<0.05$, **, $p<0.01$ vs. the indicated group).

1α), but not in luciferase-shRNA (shLuci) transfected cells, and the inhibition of AMPK-1α expression did not affect the expression of PFK2 (Fig. 6B). After treatment of shAMPK-1α-transfected cells with 250 μM H_2O_2 for 90 min, the H_2O_2-induced phosphorylation of AMPK-1α and PFK2 was abolished at 72 h and the H_2O_2-induced increase in the rate of [^{3}H]-2DG uptake was diminished at 72 h (Fig. 6B). Besides, the H_2O_2-induced increase of lactate production was also attenuated in cells pre-treated with 20 μM AMPKi for 1 h and in shAMPK-1α-transfected cells, respectively (Fig. 6C). Furthermore, by using Seahorse XF24 Analyzer, we confirmed that the

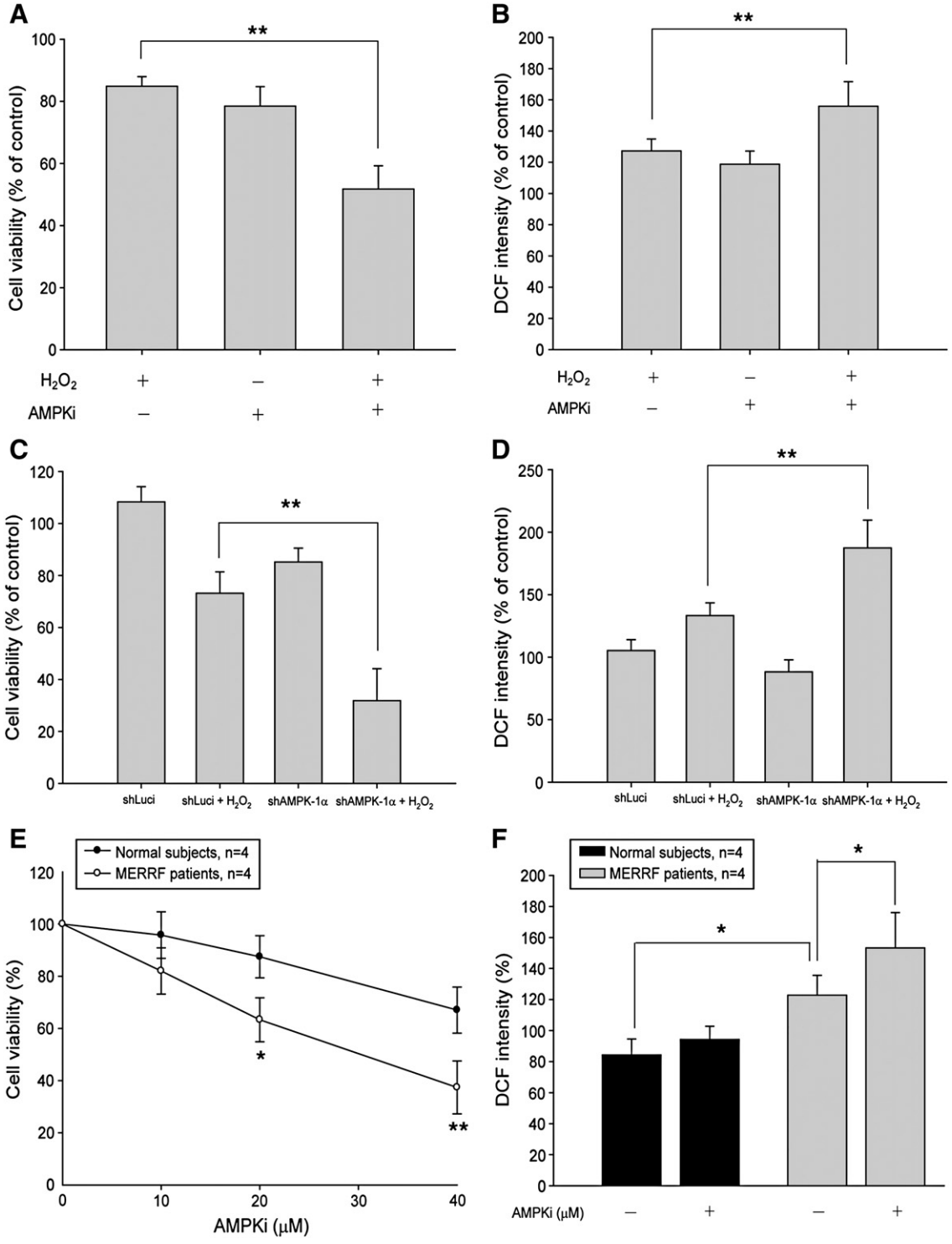

Fig. 7. Essential role of AMPK activation for the survival of H_2O_2-treated normal skin fibroblasts and MERRF skin fibroblasts. (A and C) After inhibition of AMPK activation in CCD966SK cells by pre-treatment with AMPKi for 1 h and by knockdown of AMPK-1α gene, respectively, followed by addition of 250 μM H_2O_2 for 90 min, the cell viability and (B and D) the intracellular H_2O_2 content were measured at 72 h. (E) After treatment of the primary culture of skin fibroblasts from normal subjects (n = 4) and MERRF patients (n = 4) with 10, 20 and 40 μM AMPKi for 24 h, the cell viability was determined, respectively. (F) The mean values of the intracellular H_2O_2 contents were determined in the primary culture of skin fibroblasts from normal subjects (n = 4) and MERRF patients (n = 4), respectively, after treatment of the cells with 20 μM AMPKi for 24 h. Data are presented as means ± S.D. of the results from three independent experiments (*, $p<0.05$, **, $p<0.01$ vs. the indicated group).

H_2O_2-induced increase of ECAR was abolished in the cells with AMPK-1α knockdown as compared with the scramble control (Supplementary Fig. 3). On the other hand, we showed that after inhibition of AMPK in the primary culture of skin fibroblasts by 20 μM AMPKi for 24 h, the rate of lactate production in MERRF skin fibroblasts (n = 4) was substantially decreased, but there was no such change in skin fibroblasts from age-matched normal subjects (n = 4) (Fig. 6D).

3.5. AMPK-mediated increase of glycolytic flux in oxidative stressed skin fibroblasts

To examine the essential role of AMPK activation in skin fibroblasts to cope with oxidative stress, we had pre-treated CCD-966SK cells with 20 μM AMPKi for 1 h followed by addition of 250 μM H_2O_2 for 90 min, and then determined the cell viability and intracellular ROS level at 72 h. The results showed that cells with inactivated AMPK were far more sensitive to H_2O_2-induced oxidative stress, which resulted in significant decrease of cell viability and increase of the intracellular ROS level (Fig. 7A and B). Likewise, the cell viability was also substantially decreased in shAMPK-1α-transfected cells by exposure to 250 μM H_2O_2, which were accompanied by an elevation of intracellular ROS level (Fig. 7C and D). On the other hand, we showed that after inhibition of AMPK in the primary culture of skin fibroblasts from MERRF patients (n = 4) and normal subjects (n = 4) by treatment with AMPKi (10, 20 and 40 μM) for 24 h, MERRF skin fibroblasts became more susceptible to death as compared with normal skin fibroblasts (Fig. 7E). Besides, the intracellular H_2O_2 content was increased in MERRF skin fibroblasts after treatment of the cells with 20 μM AMPKi for 24 h, but there was no such change in skin fibroblasts from normal subjects (Fig. 7F).

3.6. AMPK-mediated increase of the glycolytic flux contributed to the elevation of intracellular NADPH in H_2O_2-treated normal skin fibroblasts and MERRF skin fibroblasts

It has been reported that the redistribution of glucose metabolites can regulate the intracellular NADPH production via PPP [21,22]. We then investigated whether AMPK-mediated increase of glycolytic flux in skin fibroblasts could contribute to an increase of the intracellular NADPH. We first observed that enhanced glycolytic flux by H_2O_2 was accompanied by an increase of intracellular NADPH content in CCD-966SK cells, but the H_2O_2-induced increase of intracellular NADPH content was diminished in CCD-966SK cells that were treated with 200 μM 6-aminonicotinamide (6AN, a G6PD inhibitor) (Fig. 8A). In addition, we inhibited glycolytic flux either by culture of CCD-966SK cells in a glucose-free medium containing 5 mM galactose or by pre-treatment of CCD-966SK cells with 20 μM AMPKi for 1 h, the H_2O_2-induced increase of intracellular NADPH content was abolished at 72 h (Fig. 8A). Furthermore, an increase in the intracellular NADPH content by H_2O_2 was abrogated in shAMPK-1α-transfected cells as compared with shLuci-transfected cells (Fig. 8B). On the other hand, we showed that the intracellular NADPH content in MERRF skin fibroblasts (n = 4) was higher than those of the skin fibroblasts from normal subjects (n = 4). After treatment of MERRF skin fibroblasts with 20 μM AMPKi for 24 h, the intracellular NADPH content was significantly decreased, but there was no obvious change in the skin fibroblasts from normal subjects (n = 4) (Fig. 8C).

3.7. Up-regulation of NADPH-mediated antioxidant enzymes expression and GSH level in H_2O_2-treated normal skin fibroblasts and MERRF skin fibroblasts

To examine whether H_2O_2-induced increase of NADPH level affected the antioxidant capacity, we investigated the protein expression levels of NADPH-dependent antioxidant enzymes including

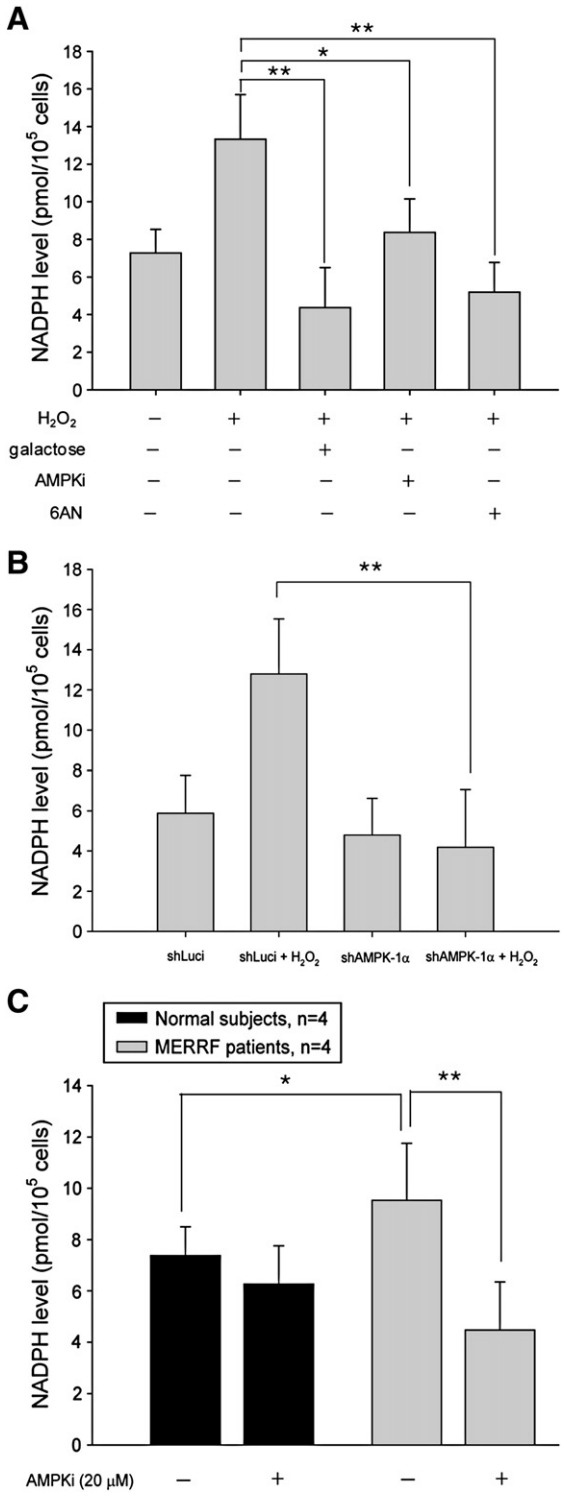

Fig. 8. Regulation of intracellular NADPH production by AMPK in H_2O_2-treated normal skin fibroblasts and in MERRF skin fibroblasts. (A) After induction of oxidative stress by 250 μM H_2O_2 at 24 h, CCD-966SK cells were incubated either with 5 mM galactose in a glucose-free medium or 200 μM 6-AN (a G6PD inhibitor) for another 48 h to determine the intracellular NADPH content. After inhibition of AMPK activation in CCD-966SK cells by pre-treatment of the cells with 20 μM AMPKi for 1 h or (B) by knockdown of AMPK-1α gene followed by treatment of the cells with 250 μM H_2O_2 for 90 min, the intracellular NADPH content was measured at 72 h. (C) The mean value of intracellular NADPH level was determined for the primary culture of skin fibroblasts from normal subjects (n = 4) and MERRF patients (n = 4), respectively, after treatment of the cells with 20 μM AMPKi for 24 h. Data are presented as means ± S.D. of the results from three independent experiments (*, $p<0.05$, **, $p<0.01$ vs. the indicated group).

glutathione peroxide 1(GPx-1), glutathione reductase (GR), thioredoxin 1 (Trx-1) and peroxiredoxin 1 (Prx-1) in H_2O_2-treated CCD-966SK cells. The results showed that GPx-1, GR, Trx-1 and Prx-1 were up-regulated at 72 h after addition of CCD-966SK cells to 250 μM H_2O_2 (Fig. 9A). Besides, we also found that H_2O_2-induced GSH production was reduced in 6-AN-treated cells and in transfected cells with AMPK-1α knockdown, respectively (Fig. 9B). Significantly, we showed that the intracellular GSH contents in MERRF skin fibroblasts (n = 4) were higher than those of the normal controls (n = 4), but this increase was suppressed by treatment of cells with 20 μM AMPKi for 24 h (Fig. 9C).

4. Discussion

In this study, we showed for the first time that the energy metabolism in MERRF skin fibroblasts was more dependent on anaerobic glycolysis as compared with the skin fibroblasts from age-matched normal subjects by using the Seahorse XF24 Analyzer (Fig. 1). Clinically, the levels of lactate and pyruvate in serum from patients with MERRF syndrome are often elevated at rest and increased excessively after moderate exercise [32]. Our findings are also in agreement with previous reports that transmitochondrial cytoplasmic hybrid cells (cybrids) with a pathogenic mtDNA mutation were highly dependent on anaerobic glycolysis for energy supply [33–35]. Most importantly, we found that the phosphorylation of AMPK-1α and PFK2, one of the main regulatory steps in glycolysis, were up-regulated in MERRF skin fibroblasts as compared to the skin fibroblasts from age-matched normal subjects (Fig. 5E). The activation of AMPK in MERRF skin fibroblasts was involved in the regulation of the intracellular NADPH and GSH production (Figs. 8C and 9C). It is noteworthy that intracellular GSH content was reported to be increased in affected tissues of MERRF patients and may be considered as an initial sign of respiratory chain dysfunction [36].

It has been demonstrated that human cells exhibit a broad spectrum of responses to oxidative stress, depending on the stress

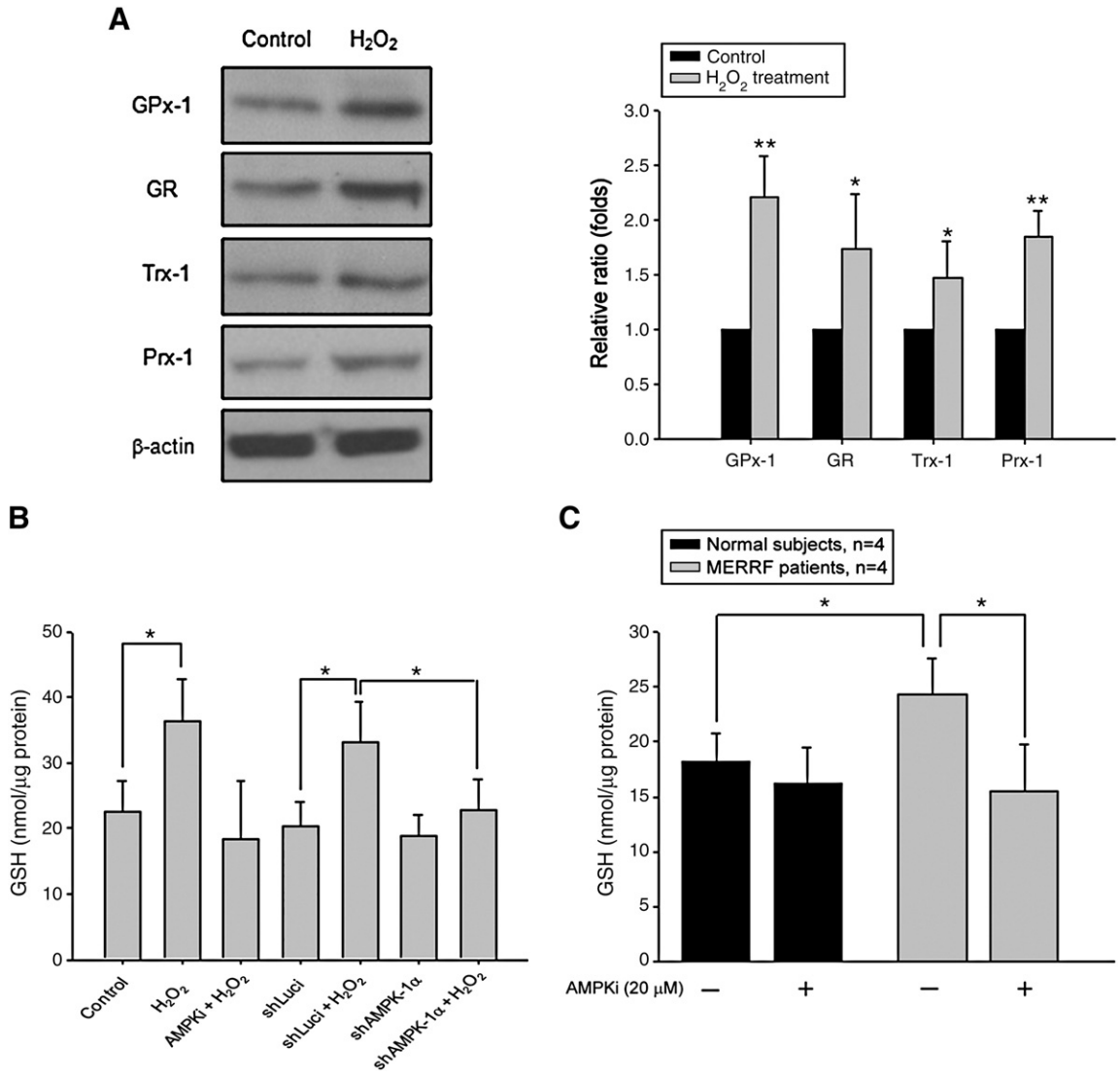

Fig. 9. Up-regulation of NADH-mediated antioxidant system in H_2O_2-treated normal skin fibroblasts and in MERRF skin fibroblasts. (A) After treatment of CCD-966SK cells with 250 μM H_2O_2 for 90 min, the expression levels of proteins including GPx-1, GR, Trx-1 and Prx-1 were determined by Western blot. By densitometric analysis from three independent Western blots, the proteins expression levels in CCD-966SK cells were normalized to the β-actin expression level, and the results are shown in the right panel. (B) After induction of oxidative stress by addition of 250 μM H_2O_2 at 24 h, CCD-966SK cells were incubated with 200 μM 6AN for another 48 h to determine the intracellular GSH level. The intracellular GSH level was also examined in shLuci-transfected and shAMPK-1α-transfected cells after addition to 250 μM H_2O_2 at 72 h. (C) After treatment of the cells with 20 μM AMPKi for 24 h, the mean value of intracellular GSH level for the primary culture of skin fibroblasts from normal subjects (n = 4) and MERRF patients (n = 4) were determined. Data are presented as means ± S.D. of the results from three independent experiments (*, $p<0.05$, ** $p<0.01$ vs. the indicated group).

level [37]. In the present study, we treated CCD-966SK cells with a sub-lethal dose of H_2O_2 for a short time to induce oxidative stress, in which no apoptotic cells were observed. However, the intracellular ROS level was increased to 1.27-fold and the doubling-time of skin fibroblasts was increased from 32.7 ± 2.2 h (control) to 43.2 ± 5.1 h (H_2O_2-treated). It is noteworthy that oxidative stress plays a vital role in affected tissues of MERRF patients who usually display slow deteriorating clinical courses [38,39]. Therefore, examination of the cellular response to oxidative stress induced by a sub-lethal dose of H_2O_2 can provide useful information to unravel the molecular basis of the pathophysiology of mitochondrial diseases or age-related neurodegenerative diseases [11,40–42]. In addition, a better understanding of the oxidative stress response of human cells is of clinical importance in therapeutic interventions of the disease progression.

We demonstrated for the first time that the AMPK-mediated increase of glycolysis in skin fibroblasts was essential for the survival of cells under oxidative stress (Fig. 10). Although our findings are in line with the previous reports that AMPK-mediated activation of glycolysis was required for the protection of astrocytes and cardiomyocytes, respectively against oxidative stress [43,44], the action mechanism of AMPK in cells under oxidative stress has remained equivocal. Cao and coworkers demonstrated that persistent treatment of skin fibroblast with 250 μM H_2O_2 for 24 h, the AMPK activation by ROS caused the inhibition of the mammalian target of rapamycin (mTOR) signaling that led to apoptosis of skin fibroblasts [45]. Therefore, we consider that the roles that AMPK played may be dictated by the degree of intracellular ROS contents.

It was reported that the intracellular NADPH production was effected by G6PD [46,47]. The expression of G6PD was regulated by oxidants-induced oxidative stress due to the presence of an oxidative stress response element in the promoter region of the G6PD gene, which is similar to that found in manganese-containing superoxide dismutase (Mn-SOD) [48]. Nevertheless, the up-regulation of G6PD protein expression by H_2O_2 was observed in shAMPK-1α-transfected cells suggesting that the expression of G6PD was not regulated by AMPK (Supplementary Fig. 4). In light of the recent report that the G6PD activity can be regulated by reversible tyrosine phosphorylation [49], whether AMPK can activate the G6PD by post-translational modification to increase NADPH production is worthy of further investigation.

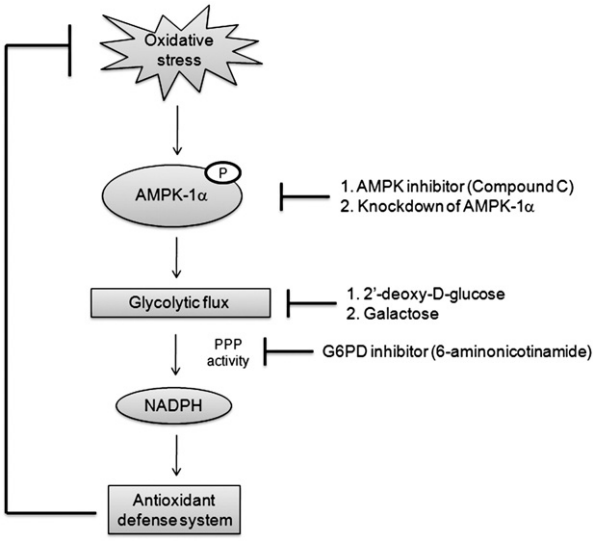

Fig. 10. A proposed scheme of AMPK activation for the cell survival under oxidative stress. Under oxidative stress, AMPK is activated to trigger the glycolytic flux, which contributes to the increased production of NADPH via the PPP in human skin fibroblasts. The AMPK-mediated increase of intracellular NADPH level, a major source of the reducing equivalents, further participates in the antioxidant defense system to counteract the oxidative stress for cell survival.

Although glycolysis and PPP are parallel pathways in glucose metabolism, the redistribution of glycolytic flux can regulate the PPP activity for the generation of NADPH [21,22]. The findings of this study further suggest that the increase of glycolytic flux exerted by AMPK activation can regulate the intracellular NADPH production. On the other hand, the intracellular NADH level was increased in both shAMPK-1α-transfected cells and scramble controls after treatment with H_2O_2, which suggested that the generation of NADH was not regulated by AMPK (Supplementary Fig. 5A). Indeed, under the normal glycolytic flux, pyruvate conversion into lactate by LDH at the expense of oxidation of NADH can recover NAD^+ in the cytosol for glycolysis to continue. Besides, we consider that the increase of NADH level in H_2O_2-treated normal skin fibroblasts may be resulted from defective mitochondria, which decreased the utilization of NADH substrate. Accordingly, we observed that the NADH level in MERRF skin fibroblasts was higher than that of the skin fibroblasts of normal subjects, but was not altered by treatment with AMPK inhibitor (Supplementary Fig. 5B).

Glycolysis is well-regulated by a coordination of several transcription factors including AMPK, AKT, c-MYC, HIF-1α and p53 [50–52]. In addition, the up-regulation of glucose transporter, glycolytic enzymes and regulatory enzymes are also required for the increase of glycolytic activity. In this study, we observed that several glycolytic enzymes (GLUT1, HKII, PFK1 and LDH) were up-regulated in H_2O_2-treated normal skin fibroblasts at 24 h, but the glycolytic flux were significantly increased at 48 and 72 h. This phenomenon could be explained by a scenario that the metabolic shift to glycolysis in skin fibroblasts is a gradual process after treatment of cells with a sub-lethal dose of H_2O_2. Recently, it has been reported that AMPK can up-regulate the protein expression of GLUT1 in epithelial cells to stimulate glycolysis in response to inhibition of OXPHOS [53]. Therefore, whether AMPK-mediated increased of glycolytic flux in skin fibroblasts could be regulated by its direct/indirect up-regulation of the expression of GLUT1 or other glycolytic enzymes remains to be further examined.

On the other hand, recent studies have suggested that activation of AMPK is involved in the up-regulation of several antioxidant enzymes [54,55]. AMPK can directly phosphorylate the forkhead transcription factor (FOXO) to promote its nuclear translocation and the formation of subsequent transcription activation complex [56]. The activation of the AMPK–FOXO pathway can reduce oxidant-induced ROS production by up-regulating the expression of thioredoxin and peroxiredoxin [57,58]. Our previous studies revealed that several antioxidant enzymes were up-regulated in MERRF skin fibroblasts [2,11]. Therefore, whether the activation of AMPK in MERRF skin fibroblasts is involved in the up-regulation of antioxidant enzymes warrants further investigation.

In conclusion, we have demonstrated that AMPK is involved in the up-regulation of the glycolytic flux and contributes to the increased production of NADPH via the PPP, which is essential for the survival of MERRF skin fibroblasts and H_2O_2-treated normal skin fibroblasts (Fig. 10). The findings of this study have provided new information for us to better understand the response to oxidative stress of human skin fibroblasts and shed a new light in unraveling the molecular basis of the pathophysiology of mitochondrial diseases such as MERRF syndrome.

Supplementary materials related to this article can be found online at doi:10.1016/j.bbadis.2011.09.014.

List of abbreviations

MERRF	myoclonic epilepsy and ragged-red fibers
OCR	oxygen consumption rate
ECAR	extracellular acidification rate
ROS/RNS	reactive oxygen/nitrogen species
AMPK	AMP-activated protein kinase

PPP	pentose phosphate pathway
NADPH	reduced nicotinamide adenine dinucleotide phosphate
GSH	glutathione
2DG	2′-deoxy-D-glucose
AnA	antimycin A
NAC	*N*-acetylcysteine
AMPKi	AMPK inhibitor
shLuci	shRNA for luciferase gene
shAMPK-1α	shRNA for AMPK-1α gene

Acknowledgements

This work was supported by grants from National Science Council (NSC96-2320-B-010-006 and NSC97-2320-B-010-038-MY3), Executive Yuan, Taiwan. It was partly supported by an intramural grant (No. 982A01) from Mackay Medical College. The authors would like to express their appreciation of the technical support and service of the Core Facilities at National Yang-Ming University.

References

[1] D.C. Wallace, Mitochondrial diseases in man and mouse, Science 283 (1999) 1482–1488.
[2] Y.S. Ma, Y.C. Chen, C.Y. Lu, C.Y. Liu, Y.H. Wei, Upregulation of matrix metalloproteinase 1 and disruption of mitochondrial network in skin fibroblasts of patients with MERRF syndrome, Ann. N. Y. Acad. Sci. 1042 (2005) 55–63.
[3] A.M. James, Y.H. Wei, C.Y. Pang, M.P. Murphy, Altered mitochondrial function in fibroblasts containing MELAS or MERRF mitochondrial DNA mutations, Biochem. J. 318 (1996) 401–407.
[4] W.K. Porteous, A.M. James, P.W. Sheard, C.M. Porteous, M.A. Packer, S.J. Hyslop, J.V. Melton, C.Y. Pang, Y.H. Wei, M.P. Murphy, Bioenergetic consequences of accumulating the common 4977-bp mitochondrial DNA deletion, Eur. J. Biochem. 257 (1998) 192–201.
[5] J.M. Shoffner, M.T. Lott, A.M. Lezza, P. Seibel, S.W. Ballinger, D.C. Wallace, Myoclonic epilepsy and ragged-red fiber disease (MERRF) is associated with a mitochondrial DNA $tRNA^{Lys}$ mutation, Cell 61 (1990) 931–937.
[6] J.A. Enriquez, A. Chomyn, G. Attardi, MtDNA mutation in MERRF syndrome causes defective aminoacylation of $tRNA^{Lys}$ and premature translation termination, Nat. Genet. 10 (1995) 47–55.
[7] H. Antonická, D. Floryk, P. Klement, L. Stratilová, J. Hermanská, H. Houstková, M. Kalous, Z. Drahota, J. Zeman, J. Houstek, Defective kinetics of cytochrome *c* oxidase and alteration of mitochondrial membrane potential in fibroblasts and cytoplasmic hybrid cells with the mutation for myoclonus epilepsy with ragged-red fibres (MERRF) at position 8344 nt, Biochem. J. 342 (1999) 537–544.
[8] C. Vives-Bauza, R. Gonzalo, G. Manfredi, E. Garcia-Arumi, A.L. Andreu, Enhanced ROS production and antioxidant defenses in cybrids harbouring mutations in mtDNA, Neurosci. Lett. 391 (2006) 136–141.
[9] S.B. Wu, Y.S. Ma, Y.T. Wu, Y.C. Chen, Y.H. Wei, Mitochondrial DNA mutation-elicited oxidative stress, oxidative damage, and altered gene expression in cultured cells of patients with MERRF syndrome, Mol. Neurobiol. 41 (2010) 256–266.
[10] H.C. Lee, P.H. Yin, C.W. Chi, Y.H. Wei, Increase in mitochondrial mass in human fibroblasts under oxidative stress and during replicative cell senescence, J. Biomed. Sci. 9 (2002) 517–526.
[11] C.F. Lee, Y.C. Chen, C.Y. Liu, Y.H. Wei, Involvement of protein kinase C delta in the alteration of mitochondrial mass in human cells under oxidative stress, Free Radic. Biol. Med. 40 (2006) 2136–2146.
[12] C. Cantó, J. Auwerx, AMP-activated protein kinase and its downstream transcriptional pathways, Cell. Mol. Life Sci. 67 (2010) 3407–3423.
[13] D.G. Hardie, The AMP-activated protein kinase pathway-new players upstream and downstream, J. Cell Sci. 117 (2004) 5479–5487.
[14] S.A. Hawley, M. Davison, A. Woods, S.P. Davies, R.K. Beri, D. Carling, D.G. Hardie, Characterization of the AMP-activated protein kinase kinase from rat liver and identification of threonine 172 as the major site at which it phosphorylates AMP-activated protein kinase, J. Biol. Chem. 271 (1996) 27879–27887.
[15] M.J. Birnbaum, Activating AMP-activated protein kinase without AMP, Mol. Cell 19 (2005) 289–290.
[16] Z. Luo, A.K. Saha, X. Xiang, N.B. Ruderman, AMPK, the metabolic syndrome and cancer, Trends Pharmacol. Sci. 26 (2005) 69–76.
[17] Y. Han, Q. Wang, P. Song, Y. Zhu, M.H. Zou, Redox regulation of the AMP-activated protein kinase, PLoS One 5 (2010) e15420.
[18] S.L. Choi, S.J. Kim, K.T. Lee, J. Kim, J. Mu, M.J. Birnbaum, S. Soo Kim, J. Ha, The regulation of AMP-activated protein kinase by H_2O_2, Biochem. Biophys. Res. Commun. 287 (2001) 92–97.
[19] C. Cao, S. Lu, Q. Jiang, W.J. Wang, X. Song, R. Kivlin, B. Wallin, A. Bagdasarian, T. Tamakloe, W.M. Chu, J. Marshall, N. Kouttab, A. Xu, Y. Wan, EGFR activation confers protections against UV-induced apoptosis in cultured mouse skin dendritic cells, Cell. Signal. 20 (2008) 1830–1838.
[20] P. Cidad, A. Almeida, J.P. Bolaños, Inhibition of mitochondrial respiration by nitric oxide rapidly stimulates cytoprotective GLUT3-mediated glucose uptake through 5′-AMP-activated protein kinase, Biochem. J. 384 (2004) 629–636.
[21] C. Le Goffe, G. Vallette, L. Charrier, T. Candelon, C. Bou-Hanna, J.F. Bouhours, C.L. Laboisse, Metabolic control of resistance of human epithelial cells to H_2O_2 and NO stresses, Biochem. J. 364 (2002) 349–359.
[22] D. Schubert, Glucose metabolism and Alzheimer's disease, Ageing Res. Rev. 4 (2005) 240–257.
[23] S. Filosa, A. Fico, F. Paglialunga, M. Balestrieri, A. Crooke, P. Verde, P. Abrescia, J.M. Bautista, G. Martini, Failure to increase glucose consumption through the pentose-phosphate pathway results in the death of glucose-6-phosphate dehydrogenase gene-deleted mouse embryonic stem cells subjected to oxidative stress, Biochem. J. 370 (2003) 935–943.
[24] A. Fico, F. Paglialunga, L. Cigliano, P. Abrescia, P. Verde, G. Martini, I. Iaccarino, S. Filosa, Glucose-6-phosphate dehydrogenase plays a crucial role in protection from redox-stress-induced apoptosis, Cell Death Differ. 11 (2004) 823–831.
[25] E.V. Kalinina, N.N. Chernov, A.N. Saprin, Involvement of thio-, peroxi-, and glutaredoxins in cellular redox-dependent processes, Biochemistry 73 (2008) 1493–1510.
[26] J.M. Myers, C.R. Myers, The effects of hexavalent chromium on thioredoxin reductase and peroxiredoxins in human bronchial epithelial cells, Free Radic. Biol. Med. 47 (2009) 1477–1485.
[27] C. Le Goffe, G. Vallette, A. Jarry, C. Bou-Hanna, C.L. Laboisse, The in vitro manipulation of carbohydrate metabolism: a new strategy for deciphering the cellular defence mechanisms against nitric oxide attack, Biochem. J. 344 (1999) 643–648.
[28] A.A. Gerencser, A. Neilson, S.W. Choi, U. Edman, N. Yadava, R.J. Oh, D.A. Ferrick, D.G. Nicholls, M.D. Brand, Quantitative microplate-based respirometry with correction for oxygen diffusion, Anal. Chem. 81 (2009) 6868–6878.
[29] C.Y. Liu, C.F. Lee, Y.H. Wei, Activation of PKCdelta and ERK1/2 in the sensitivity to UV-induced apoptosis of human cells harboring 4977 bp deletion of mitochondrial DNA, Biochim. Biophys. Acta 1792 (2009) 783–790.
[30] C.T. Chen, Y.R. Shih, T.K. Kuo, O.K. Lee, Y.H. Wei, Coordinated changes of mitochondrial biogenesis and antioxidant enzymes during osteogenic differentiation of human mesenchymal stem cells, Stem Cells 26 (2008) 960–968.
[31] A.S. Marsin, L. Bertrand, M.H. Rider, J. Deprez, C. Beauloye, M.F. Vincent, G. van den Berghe, D. Carling, L. Hue, Phosphorylation and activation of heart PFK-2 by AMPK has a role in the stimulation of glycolysis during ischemia, Curr. Biol. 10 (2000) 1247–1255.
[32] T.D. Sanger, K.D. Jain, MERRF syndrome with overwhelming lactic acidosis, Pediatr. Neurol. 14 (1996) 57–61.
[33] J.C. von Kleist-Retzow, H.T. Hornig-Do, M. Schauen, S. Eckertz, T.A. Dinh, F. Stassen, N. Lottmann, M. Bust, B. Galunska, K. Wielckens, W. Hein, J. Beuth, J.M. Braun, J.H. Fischer, V.Y. Ganitkevich, K. Maniura-Weber, R.J. Wiesner, Impaired mitochondrial Ca^{2+} homeostasis in respiratory chain-deficient cells but efficient compensation of energetic disadvantage by enhanced anaerobic glycolysis due to low ATP steady state levels, Exp. Cell Res. 313 (2007) 3076–3089.
[34] F. Pallotti, A. Baracca, E. Hernandez-Rosa, W.F. Walker, G. Solaini, G. Lenaz, G.V. Melzi D'Eril, S. Dimauro, E.A. Schon, M.M. Davidson, Biochemical analysis of respiratory function in cybrid cell lines harbouring mitochondrial DNA mutations, Biochem. J. 384 (2004) 287–293.
[35] A. Hansson, N. Hance, E. Dufour, A. Rantanen, K. Hultenby, D.A. Clayton, R. Wibom, N.G. Larsson, A switch in metabolism precedes increased mitochondrial biogenesis in respiratory chain-deficient mouse hearts, Proc. Natl. Acad. Sci. U. S. A. 101 (2004) 3136–3141.
[36] M. Filosto, P. Tonin, G. Vattemi, M. Spagnolo, N. Rizzuto, G. Tomelleri, Antioxidant agents have a different expression pattern in muscle fibers of patients with mitochondrial diseases, Acta Neuropathol. 103 (2002) 215–220.
[37] D.R. Crawford, K.J. Davies, Adaptive response and oxidative stress, Environ. Health Perspect. 10 (1994) 25–28.
[38] C.C. Huang, H.C. Kuo, C.C. Chu, C.W. Liou, Y.S. Ma, Y.H. Wei, Clinical phenotype, prognosis and mitochondrial DNA mutation load in mitochondrial encephalomyopathies, J. Biomed. Sci. 9 (2002) 527–533.
[39] W. Fan, K.G. Waymire, N. Narula, P. Li, C. Rocher, P.E. Coskun, M.A. Vannan, J. Narula, G.R. Macgregor, D.C. Wallace, A mouse model of mitochondrial disease reveals germline selection against severe mtDNA mutations, Science 319 (2008) 958–962.
[40] L. Tretter, V. Adam-Vizi, Inhibition of Krebs cycle enzymes by hydrogen peroxide: a key role of [alpha]-ketoglutarate dehydrogenase in limiting NADH production under oxidative stress, J. Neurosci. 20 (2000) 8972–8979.
[41] A.C. Nulton-Persson, L.I. Szweda, Modulation of mitochondrial function by hydrogen peroxide, J. Biol. Chem. 276 (2001) 23357–23361.
[42] J.K. Ngo, K.J. Davies, Mitochondrial Lon protease is a human stress protein, Free Radic. Biol. Med. 46 (2009) 1042–1048.
[43] A. Almeida, S. Moncada, J.P. Bolaños, Nitric oxide switches on glycolysis through the AMP protein kinase and 6-phosphofructo-2-kinase pathway, Nat. Cell Biol. 6 (2004) 45–51.
[44] R.R. Russell III, J. Li, D.L. Coven, M. Pypaert, C. Zechner, M. Palmeri, F.J. Giordano, J. Mu, M.J. Birnbaum, L.H. Young, AMP-activated protein kinase mediates ischemic glucose uptake and prevents postischemic cardiac dysfunction, apoptosis, and injury, J. Clin. Invest. 114 (2004) 495–503.
[45] C. Cao, S. Lu, R. Kivlin, B. Wallin, E. Card, A. Bagdasarian, T. Tamakloe, W.M. Chu, K.L. Guan, Y. Wan, AMP-activated protein kinase contributes to UV- and H_2O_2-induced apoptosis in human skin keratinocytes, J. Biol. Chem. 283 (2008) 28897–28908.

[46] W.N. Tian, L.D. Braunstein, K. Apse, J. Pang, M. Rose, X. Tian, R.C. Stanton, Importance of glucose-6-phosphate dehydrogenase activity in cell death, Am. J. Physiol. 276 (1999) C1121–C1131.
[47] M.E. Tome, D.B. Johnson, B.K. Samulitis, R.T. Dorr, M.M. Briehl, Glucose 6-phosphate dehydrogenase overexpression models glucose deprivation and sensitizes lymphoma cells to apoptosis, Antioxid. Redox Signal. 8 (2006) 1315–1327.
[48] R.F. Kletzien, P.K. Harris, L.A. Foellmi, Glucose-6-phosphate dehydrogenase: a "housekeeping" enzyme subject to tissue-specific regulation by hormones, nutrients, and oxidant stress, FASEB J. 8 (1994) 174–181.
[49] S. Pan, C.J. World, C.J. Kovacs, B.C. Berk, Glucose 6-phosphate dehydrogenase is regulated through c-Src-mediated tyrosine phosphorylation in endothelial cells, Arterioscler. Thromb. Vasc. Biol. 29 (2009) 895–901.
[50] L. Hue, M.H. Rider, Role of fructose 2,6-bisphosphate in the control of glycolysis in mammalian tissues, Biochem. J. 245 (1987) 313–324.
[51] S.J. Pilkis, T.H. Claus, I.J. Kurland, A.J. Lange, 6-Phosphofructo-2-kinase / fructose-2, 6-bisphosphatase: a metabolic signaling enzyme, Annu. Rev. Biochem. 64 (1995) 799–835.
[52] S.J. Yeung, J. Pan, M.H. Lee, Roles of p53, MYC and HIF-1 in regulating glycolysis — the seventh hallmark of cancer, Cell. Mol. Life Sci. 65 (2008) 3981–3999.
[53] M. Jing, F. Ismail-Beigi, Critical role of 5′-AMP-activated protein kinase in the stimulation of glucose transporter in response to inhibition of oxidative phosphorylation, Am. J. Physiol. Cell Physiol. 292 (2007) 477–487.
[54] V.C. Calegari, C.C. Zoppi, L.F. Rezende, L.R. Silveira, E.M. Carneiro, A.C. Boschero, Endurance training activates AMP-activated protein kinase, increases expression of uncoupling protein 2 and reduces insulin secretion from rat pancreatic islets, J. Endocrinol. 208 (2011) 257–264.
[55] S.L. Colombo, S. Moncada, AMPK-1a regulates the antioxidant status of vascular endothelial cells, Biochem. J. 421 (2009) 163–169.
[56] E.L. Greer, D. Dowlatshahi, M.R. Banko, J. Villen, K. Hoang, D. Blanchard, S.P. Gygi, A. Brunet, An AMPK–FOXO pathway mediates longevity induced by a novel method of dietary restriction in *C. elegans*, Curr. Biol. 17 (2007) 1646–1656.
[57] X.N. Li, J. Song, L. Zhang, S.A. LeMaire, X. Hou, C. Zhang, J.S. Coselli, L. Chen, X.L. Wang, Y. Zhang, Y.H. Shen, Activation of the AMPK–FOXO3 pathway reduces fatty acid-induced increase in intracellular reactive oxygen species by upregulating thioredoxin, Diabetes 58 (2009) 2246–2257.
[58] C.B. Chiribau, L. Cheng, I.C. Cucoranu, Y.S. Yu, R.E. Clempus, D. Sorescu, FOXO3A regulates peroxiredoxin III expression in human cardiac fibroblasts, J. Biol. Chem. 283 (2008) 8211–8217.